ELSEVIER

International Journal of Pharmaceutics 161 (1998) 225–236

international journal of pharmaceutics

Internal and external structure of pellets made in a rotary processor

J. Vertommen *, P. Rombaut, R. Kinget

Laboratorium voor Farmacotechnologie en Biofarmacie, Katholieke Universiteit Leuven, Campus Gasthuisberg O + N, Herestraat 49, B-3000 Leuven, Belgium

Received 22 July 1997; received in revised form 23 October 1997; accepted 26 October 1997

Abstract

The internal and external structure of pellets made in a rotary processor by the wet granulation technique was studied using the following techniques: helium pycnometry to determine the true density, krypton adsorption to determine the specific surface area, mercury porosimetry, and scanning electron microscopy. The results of the true density measurements, specific surface area determinations and mercury porosimetry led to the hypothesis that the pellets were open porous sponge structures. Mercury mainly intruded in the macropore range (pores with a radius between 7 and 0.05 μm). The pores and cavities were partially closed as spheronization went on leading to air pockets in the pellets. Scanning electron microscopic pictures provided visual support for the hypothesis that the pellets had a porous surface and that the pellets contained cavities, which could be closed resulting in the formation of air pockets. To reduce the pore volume and smooth the surface, the rotor speed should be high and the spheronization time should be long. The plastic properties of wetted microcrystalline cellulose promoted the smoothing of the surface. © 1998 Elsevier Science B.V.

Keywords: Pellets; Rotary processor; True density; Specific surface area; Mercury porosimetry

1. Introduction

Pellets are often produced using the process of extrusion and spheronization. Pelletization by the wet granulation technique in a rotary processor may be a valuable alternative to this process of extrusion and spheronization (Wan et al., 1994, 1995; Holm et al., 1996; Vertommen and Kinget, 1997). Using a rotary processor it is possible to produce, dry, and coat pellets in one piece of equipment. In this way dust problems and contamination risks can be avoided and time, equipment, energy, space, and machine operators can be saved.

* Corresponding author. Tel: + 32 16 345820; fax: + 32 16 345996; e-mail: jan.vertommen@farm.kuleuven.ac.be

PII S0378-5173(97)00357-8

To judge the quality of the pellets made in a rotary processor using the wet granulation technique with respect to further processing, it is necessary that these pellets are fully characterized. In previous papers, some of these pellet characteristics have already been described and discussed (Vertommen and Kinget, 1997; Vertommen et al., 1997). In this paper, the internal and external structure of the pellets was further investigated. Furthermore, the influence of major formulation and processing variables on the internal and external structure characteristics was studied by means of a factorial design and statistical analysis.

The first pellet characteristic which was studied in this paper was the true density. True density measurements performed on pellets made in a high shear mixer-granulator indicated the presence of air pockets in the pellets (Vertommen et al., 1994). True density measurements were, therefore, performed to investigate whether or not the pellets made in the rotary processor contained air pockets and if so, to estimate the measure of occurrence of these air pockets.

Furthermore, a knowledge of the surface area of the pellets is desirable especially if film coating of these pellets is under consideration. Because the thickness of the film applied to pellets in a sustained-release-type dosage form dictates the rate at which drug is released from the coated pellets, knowledge about the surface area to be covered cannot be overemphasized. But even in the case of non-coated pellets, knowledge about the surface area is important since drug release is influenced by the available surface area. The surface area of a pellet, assumed to be a perfect smooth sphere, can be calculated from measurement of its diameter, since the surface area of a sphere is equal to $\pi \cdot (\text{diameter})^2$. However, this calculation does not account for the contributions to the surface area arising from other morphologic characteristics, such as the porosity, the surface roughnesses and the shape of the pellets. The shape and surface roughnesses in the region of 0.03 to 0.13 times the maximum Feret diameter were determined and evaluated in a previous paper (Vertommen et al., 1997). Most pellets were evaluated as being fairly spherical and smooth. Porosity and surface roughness on a smaller scale basis had not been evaluated yet. The surface area of a pellet sample was, therefore, determined directly. Two techniques, i.e. gas adsorption (Lowell and Shields, 1991) and air permeametry (Lowell and Shields, 1991; Eriksson et al., 1993) permit direct calculation of the surface area of powders or dosage forms. A method based on the gas adsorption technique was used for the determination of the surface areas of the pellet samples. The intraparticle porosity and the presence of pores in the radius range of 0.02 to 40 μm were evaluated using mercury porosimetry (Lowell and Shields, 1991; Juppo and Yliruusi, 1994).

To allow visual confirmation of findings obtained by the true density, the surface area and the mercury porosimetry measurements, scanning electron microscopic pictures at different magnifications of some of the pellet samples were taken.

Table 1
Low and high levels for the independent variables

Independent variable	Low level	High level
(A) MCC content (%)	30	35
(B) Water-MCC ratio	1.18	1.22
(C) Rotor speed (rpm)	550	800
(D) Spheronization time (min)	5	15
(E) Water addition rate (ml/min)	30	60

Table 2
Results for the 'real' true density and the specific surface area for the powder mixtures

Experiment	'Real' true density		S^a_{BET}	
	(g/cm^3)	95% CL[b]	(m^2/g)	C-value[c]
30% MCC[d]	1.534	0.0106	0.554	147.89
35% MCC[e]	1.534	0.0140	0.605	75.19

[a] Experimentally determined specific surface area.
[b] Value, which should be added to or subtracted from the mean to obtain the 95% confidence limits ($n = 3$).
[c] BET constant.
[d] Powder mixture containing 30% microcrystalline cellulose.
[e] Powder mixture containing 35% microcrystalline cellulose.

Table 3
Results for the 'apparent' true density, experimentally determined and calculated specific surface area

Experiment	d_g^a (μm)	σ_g^b	ρ^c		S_{BET}^e		S_{calc}^g (m^2/g)
			(g/cm^3)	95% CL[d]	(m^2/g)	C-value[f]	
(1)	268	1.33	1.531	0.0029	0.522	95.38	0.0152
a	362	1.29	1.529	0.0033	0.548	28.12	0.0112
	355	1.28	1.529	0.0067	0.521	76.86	0.0114
b	363	1.34	1.528	0.0017	0.533	53.71	0.0113
ab	518	1.26	1.532	0.0064	0.513	66.97	0.00777
c	363	1.28	1.530	0.0053	0.468	70.54	0.0111
ac	503	1.27	1.531	0.0093	0.511	56.34	0.00802
bc	446	1.25	1.530	0.0078	0.511	84.01	0.00902
	387	1.25	1.529	0.0068	0.527	63.74	0.0104
abc	611	1.21	1.529	0.0050	0.439	62.88	0.00654
d	330	1.25	1.528	0.0016	0.492	68.45	0.0122
ad	393	1.25	1.536	0.0040	0.462	104.33	0.0102
bd	385	1.27	1.528	0.0025	0.489	98.19	0.0105
abd	421	1.26	1.527	0.0024	0.479	57.34	0.00959
	440	1.24	1.527	0.0061	0.510	33.19	0.00913
cd	403	1.23	1.529	0.0041	0.469	69.53	0.00995
	432	1.24	1.524	0.0017	0.543	23.72	0.00932
acd	450	1.24	1.532	0.0051	0.447	60.48	0.00891
bcd	585	1.20	1.523	0.0086	0.476	81.64	0.00684
abcd	623	1.17	1.527	0.0039	0.446	51.82	0.00639
e	372	1.33	1.531	0.0009	0.534	68.58	0.0110
ae	581	1.24	1.530	0.0072	0.538	58.34	0.00691
be	515	1.37	1.536	0.0124	0.552	36.37	0.00797
	494	1.34	1.529	0.0017	0.584	27.54	0.00829
abe	644	1.24	1.534	0.0019	0.528	50.15	0.00622
ce	441	1.26	1.531	0.0042	0.515	79.89	0.00913
ace	875	1.21	1.527	0.0009	0.427	52.82	0.00457
	935	1.18	1.524	0.0046	0.472	46.74	0.00427
bce	621	1.23	1.530	0.0015	0.492	101.09	0.00645
abce	1201	1.21	1.528	0.0032	0.389	103.82	0.00333
de	412	1.29	1.528	0.0009	0.514	43.60	0.00985
	417	1.27	1.526	0.0040	0.521	76.55	0.00970
ade	498	1.34	1.527	0.0016	0.451	68.49	0.00822
bde	447	1.27	1.526	0.0049	0.490	94.90	0.00905
abde	697	1.19	1.526	0.0016	0.421	125.94	0.00573
cde	603	1.24	1.528	0.0009	0.459	61.26	0.00666
acde	1119	1.16	1.522	0.0058	0.259	72.25	0.00356
bcde	852	1.19	1.530	0.0067	0.426	75.79	0.00468
abcde	1368	1.14	1.523	0.0060	0.323	49.25	0.00291
	1341	1.14	1.522	0.0036	0.325	50.00	0.00297

[a,b] Geometric mean diameter and geometric standard deviation on a weight basis.
[c] 'Apparent' true density.
[d] Value, which should be added to or subtracted from the mean to obtain the 95% confidence limits ($n = 3$).
[e] Experimentally determined specific surface area.
[f] BET constant.
[g] Specific surface area calculated according to Eq. (2) and Eq. (3).

2. Materials and methods

2.1. Materials

α-lactose monohydrate (Pharmatose®, type 200M, DMV, Veghel, The Netherlands), microcrystalline cellulose, abbreviated as MCC (Avicel®, type PH-101, FMC, Cork, Ireland), and riboflavin (Produits Roche, Brussel, Belgium), were used as starting materials. All materials were of Ph. Eur. grade. Purified water, Ph. Eur. grade, was used as the granulation liquid.

2.2. Methods

2.2.1. Pellet production method

The pellets were prepared in a rotary processor (MP-1 with Roto-Processor insert, Niro-Aeromatic, Bubendorf, Switzerland) by the wet granulation technique. The equipment, the preparation of the pellets, and the experimental design to evaluate the influence of major process and formulation variables were described in a previous paper (Vertommen and Kinget, 1997). For a better understanding, the independent variables with their different levels are repeated in Table 1.

2.2.2. True density

For each batch the true density was determined three times using an air-comparison pycnometer (Model 930, Beckman Instruments, Fullerton, CA, USA) with helium as the intrusive gas. Since helium penetrates into the smallest pores and crevices, it is generally conceded that the helium method gives the closest approximation to the true density.

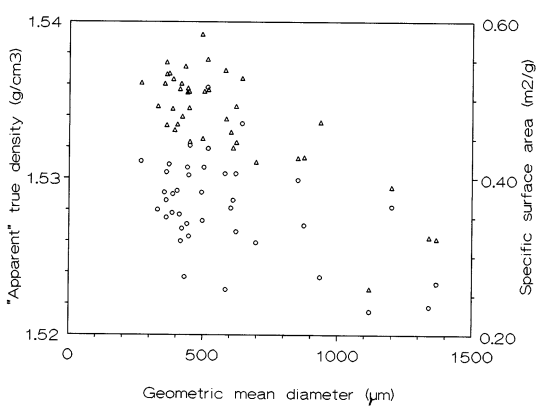

Fig. 1. 'Apparent' true density (○) and specific surface area (△) of the pellets as a function of the geometric mean diameter.

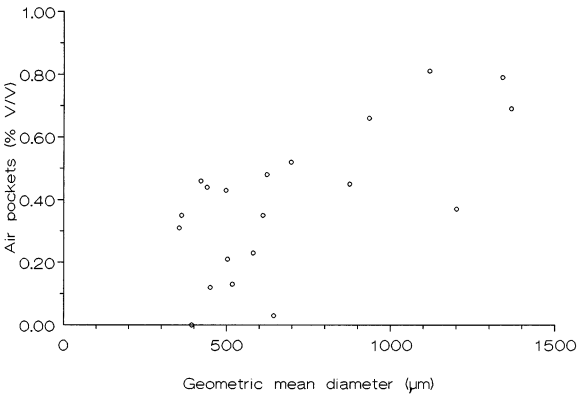

Fig. 2. Volume percentage air pockets of pellets containing 35% microcrystalline cellulose as a function of the geometric mean diameter.

Since the true density measurements of the pellets may, however, include air pockets, the results of these measurements should be called 'apparent' true densities. The 'real' true density can be determined if air pockets are excluded. This 'real' true density was obtained by measuring the true density of the powder mixtures containing 30 and 35% microcrystalline cellulose, respectively. Air pockets were assumed to be absent in the powder mixtures.

By taking the reciprocal of the true density data, 'apparent' and 'real' specific volumes were obtained. From the difference between the 'apparent' specific volume of a pellets sample and the 'real' specific volume of the corresponding powder mixture, the specific volume of the air pockets could be calculated. Hence, the volume percentage of the air pockets could be calculated using the following equation (Schmidt, 1992):

$$\%\ \text{air pockets} = \frac{\gamma_{pe} - \gamma_{pm}}{\gamma_{pe}} \cdot 100 \qquad (1)$$

γ_{pe} represents the specific volume of the pellets sample and γ_{pm} the specific volume of the corresponding powder mixture.

2.2.3. Specific surface area

Assuming that the pellets are spherical, the surface area per unit weight can be calculated (S_{calc}) from the pellet-size and the 'apparent' true density using Eq. (2) (Martin et al., 1993).

$$S_{calc} = \frac{6}{\rho \cdot d_{VS}} \quad (2)$$

where d_{VS} and ρ are the volume-surface or surface-weighted mean diameter and the 'apparent' true density of the pellets, respectively. The d_{VS} can be calculated from the geometric mean diameter (d_g) and geometric standard deviation (σ_g) on a weight basis (Vertommen and Kinget, 1997) using the following Hatch-Choate equation (Martin et al., 1993):

$$\log d_{VS} = \log d_g - 1.151 \log^2 \sigma_g \quad (3)$$

The surface area per unit weight of the pellets was experimentally determined using the dynamic method (Quantasorb® sorption system, Quantachrome, Syosset, NY, USA) with a cell having a capillary outlet and krypton as the adsorbate gas to minimize the thermal diffusion. The surface area of the sample was calculated using a 3 points BET equation (Lowell and Shields, 1991).

2.2.4. Mercury porosimetry

Mercury porosimetry is based on the Washburn equation as given in Eq. (4) (Lowell and Shields, 1991).

$$P \cdot r = -2 \cdot \gamma \cdot \cos \cdot \theta \quad (4)$$

where P is the applied pressure, r is the pore radius into which mercury will intrude, γ is the surface tension of mercury (0.480 N/m) and θ is the contact angle between mercury and the pore wall (140°). Although the apparatus (Autoscan 60, Quantachrome, Syosset, NY, USA) allowed to apply pressures up to 414 MPa, the pressure increase of interest was limited to about 40 MPa. This 40 MPa corresponded to a pore radius of about 0.02 μm. Above this pressure the pellets were likely to be compressed including the collapse of occluded pores. The compression of microcrystalline cellulose pellets at higher pressures was reported by Schröder and Kleinebudde (1995) and was indicated in this study by the fact that densities higher than the 'apparent' true densities were found if the results obtained at higher pressures were used in the calculations. Moreover, at higher pressures the surface areas calculated from the mercury porosimetry results exceeded far the ones obtained from the gas adsorption experiments.

The granule density was calculated according to Eq. (5). The granule density includes closed pores and open pores with a radius $< \approx 7$ μm.

$$\text{granule density} = \frac{W_{pe} - W_{cell}}{V_{cell} - V_{pe}} \quad (5)$$

where W_{pe} and W_{cell} are respectively the weight of the sealed cell filled with sample and the weight of the sealed empty cell. V_{pe} and V_{cell} are the volume of mercury in the cell, respectively, with and without sample.

Knowledge of the volume intruded in pores up to 0.02 μm (about 40 MPa) allowed the calculation of the apparent density, which includes closed pores and pores with a radius $< \approx 0.02$ μm (Eq. (6)).

$$\text{apparent density} = \frac{W_{pe} - W_{cell}}{V_{cell} - V_{pe} - V_{intr}} \quad (6)$$

where V_{intr} is the volume of mercury intruded in the pore range of about 7 to 0.02 μm. The intraparticle porosity of the granules was calculated from a knowledge of the 'apparent' true density and the granule density as is shown in Eq. (7):

$$\text{intraparticle porosity} = \left(1 - \frac{\text{granule density}}{\text{apparent true density}}\right) \times 100 \quad (7)$$

Pores > 7 μm in radius are commonly called megapores. In this study, megapores were defined as the pores with a radius between 40 and 7 μm. Pores with a radius between 7 μm and 0.05 μm are macropores. Pores with a radius < 0.05 μm

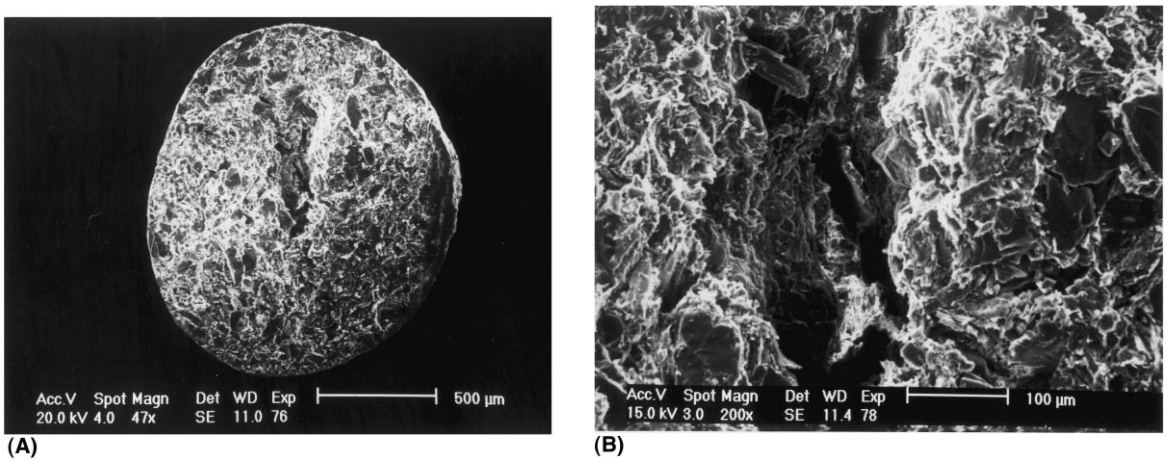

Fig. 3. Longitudinal section of a large pellet. (experiment abcde, sieve fraction 1180–1400 μm). Magnification: A = $\pm 50\times$; B = $\pm 200\times$.

are mesopores. In this study, mesopores with a radius > 0.02 μm were envisaged.

The intruded volume of mercury in each pore range, the derivative function dV/dP, the volume distribution function as a function of the radius $D_v(r)$, and the surface area distribution function as a function of the radius $D_s(r)$ were calculated from the intrusion data using the Quantachrome Autoscan PORO2PC Software, Version 3.02.

2.2.5. SEM photographs

Samples to be studied were mounted on double-sided tape on aluminium stubs, coated with gold under vacuum, and examined with a Scanning Electron Microscope (SEM FEG, XL Series, Philips Electronics, Eindhoven, The Netherlands).

2.2.6. Statistical analysis

The influence of the independent variables on the pellet characteristics ('apparent' true density and specific surface area) was analyzed by the ANOVA technique using the SOLO statistical software (SOLO Statistical System, BMDP Statistical Software, Los Angeles, CA, USA). Since second, third or fourth-order interactions are not likely to exist (Philippe, 1967), the results for these higher order interactions together with the replications were used to determine the experimental error. Using the model with main effects and first-order interactions is only valid if the residues are normally distributed. This assumption was tested by two normality tests, i.e. the Martinez-Iglewicz normality test and the Kolmogorov-Smirnov normality test.

The notation for the experiments adopted in this study is to designate any experiment in which factor A is at a high level by the corresponding lower case letter a. An experiment where factors A and B are at a higher level is thus designated ab, and the experiment where all factors are at their lower level is denoted by (Eq. (1)).

3. Results and discussion

3.1. True density

The 'real' true densities for the powder mixtures and the 'apparent' true densities for the pellets are tabulated in Tables 2 and 3. In Fig. 1, it can be seen that the geometric mean diameter and the 'apparent' true density were not strongly correlated. Nevertheless, the 'apparent' true density tended to decrease as the geometric mean diameter increased. This phenomenon, which was also observed during pelletization in a high shear mixer-granulator (Vertommen et al., 1994), may be explained as follows. All granules contain open

Table 4
Analysis of variance table for specific surface area (rounded values).

Factor or interaction	DF	Effect ($\times 10^3$)	Mean square ($\times 10^3$)	F-ratio	Prob$>F$
a	1	−43.47	16.82	30.69	<0.001
b	1	−14.77	1.96	3.58	0.071
ab	1	−11.77	1.24	2.27	0.145
c	1	−53.22	26.39	48.16	<0.001
ac	1	−18.47	3.18	5.80	0.024
bc	1	−12.70	1.45	2.65	0.117
d	1	−47.73	20.48	37.38	<0.001
ad	1	−11.23	1.13	2.07	0.164
bd	1	−4.50	0.17	0.32	0.579
cd	1	6.79	0.41	0.76	0.394
e	1	−24.59	5.64	10.29	0.004
ae	1	−23.34	5.08	9.27	0.006
be	1	−12.37	1.38	2.51	0.127
ce	1	−25.09	5.60	10.23	0.004
de	1	−19.55	3.43	6.27	0.020
error	23		0.55		

Combination acde (specific surface area of 0.259) was, based on a least squares regression, regarded as an outlier (studentized residuals), a leverage point (hat diagonals) and an influential observation (Cook's D values) and thus omitted.

pores filled with air. During further granulation and spheronization, due to a certain degree of compaction, some of these pores get closed and thus air pockets are created. Since the compaction action is stronger in the surrounding shell, the air pockets may expected to be situated in the centre, while the shell will be almost air-free. Larger pellets can contain more or larger air pockets, and they are, therefore, characterized by a lower 'apparent' true density.

Using ANOVA, it was revealed that the spheronization time was the only independent variable which influenced the 'apparent' true density significantly at the 95% confidence level ($P = 0.002$). As spheronization went on for a longer time, more of the open pores were closed, air pockets were created, and hence the 'apparent' true density decreased.

The volume percentages of air pockets for the pellets containing 35% microcrystalline cellulose, calculated according to Eq. (1), are presented in Fig. 2. The results appear to confirm the hypothesis that larger pellets contained more or larger air pockets. Although care should be taken to interpret the data absolutely, since the variation on the 'apparent' true density measurements was rather high, it was revealed that the percentage of air pockets was always low ($< 1\%$). This indicated that the pellets were open or practically open porous structures. These low percentages of air pockets contrasted with the percentages of air pockets found for pellets made in a high shear mixer-granulator, which could be calculated from true density data published before (Vertommen et al., 1994). Percentages of air pockets of $\approx 2-5\%$ were obtained for pellets containing microcrystalline cellulose and lactose. This difference can be attributed to the high compaction force delivered by the impeller of the high shear mixer-granulator compared to the relative low compaction force delivered by the rotor disk of the rotary processor.

In Fig. 3, photographs of a longitudinal section of a large pellet are presented. These photographs provided visual evidence to the hypothesis that the pellets contained cavities, which could be closed leading to the formation of air pockets. In almost every longitudinal section of a large pellet, a cavity situated near the centre was observed. The detailed picture in Fig. 3B shows the considerable dimensions of such a cavity.

3.2. Specific surface area

The experimentally determined specific surface areas of the powder mixtures are given in Table 2. The calculated and experimentally determined specific surface areas of the pellets are tabulated in Table 3. The correlation coefficients of fitting for the 3 points BET equation (1.00 for each experiment) indicated high statistical correlations. Moreover, BET constants (C-values) indicated the good reliability of the specific surface areas obtained by the BET treatment (Lowell and Shields, 1991).

The experimentally determined specific surface areas of the pellets were large compared to the calculated ones. This could be attributed to morphological characteristics such as porosity, surface roughness and shape of the pellets. Since all the pellets were fairly spherical, these large values indicated that the pellets were not completely smooth but contained roughnesses and pores.

Table 5
Densities, porosities and intruded volumes for four pellet batches

	Experiment			
	(1)	abe	acde	abcde
Granule density				
Mean (g/cm^3)	1.313	1.292	1.343	1.358
95% CL	0.0115	0.0080	0.0160	0.0052
Apparent density				
Mean (g/cm^3)	1.536	1.535	1.531	1.522
95% CL	0.0032	0.0156	0.0220	0.0119
Porosity				
Mean (%)	14.24	15.78	11.76	10.83
Megapore volume				
Mean (cm^3/g)	0.1003	0.0112	0.0059	0.0060
95% CL	0.00435	0.00262	0.00103	0.00253
Macropore volume				
Mean (cm^3/g)	0.1119	0.1221	0.0906	0.0777
95% CL	0.00401	0.00390	0.00502	0.00622
Mesopore volume				
Mean (cm^3/g)	0.0034	0.0021	0.0021	0.0031
95% CL	0.00186	0.00038	0.00114	0.00025

95% CL = value, which should be added to or subtracted from the mean to obtain the 95% confidence limits ($n = 3$).

Fractal dimensions close to two (Vertommen et al., 1997) indicated that these roughnesses were not likely to be situated in the region of 0.03–0.13 times the maximum Feret diameter. The large surface should, therefore, be attributed to surface roughnesses and pores below 8–40 μm, depending on the pellet-size.

To quantify the surface roughness linked to porosity, Faroongsarng and Peck (1994) introduced the notion Surface Irregularity Index, i.e. $1-(S_{calc}/S_{BET})$. Using the experimentally determined specific surface areas and the calculated specific surface areas (Table 3), Surface Irregularity Indices ranging from 0.971 to 0.991 can be calculated. Surface Irregularity Indices ranging from 0.78 to 0.99 were reported for some commonly used excipients (Faroongsarng and Peck, 1994). Hence, it can be concluded that the pellets exhibited high Surface Irregularity Indices, i.e. the pellets were rough due to the presence of pores.

The specific surface area decreased as the geometric mean diameter increased (Fig. 1). However, in contradistinction to what may be expected, no strong correlation could be found between the geometric mean diameter and the specific surface area.

Table 4 shows the ANOVA report for the experimentally determined specific surface area data. Significant ($P < 0.05$) interaction terms were observed between the water addition rate on the one hand and the microcrystalline cellulose content, the rotor speed or the spheronization time on the other hand. Increasing the microcrystalline cellulose content, the rotor speed or the spheronization time led to a smaller specific surface area, especially when a high water addition rate was used. At the low water addition rate, these independent variables had the same effects, but the effects were less pronounced. The interactions between the water addition rate and the microcrystalline cellulose content or the rotor speed had, however, a significant ($P \leq 0.001$) influence on the geometric mean diameter too (Vertommen and Kinget, 1997). Generally, increasing the geometric mean diameter results in a smaller specific surface area. Therefore, the influence of the interactions between the water addition rate and the microcrystalline cellulose content or the

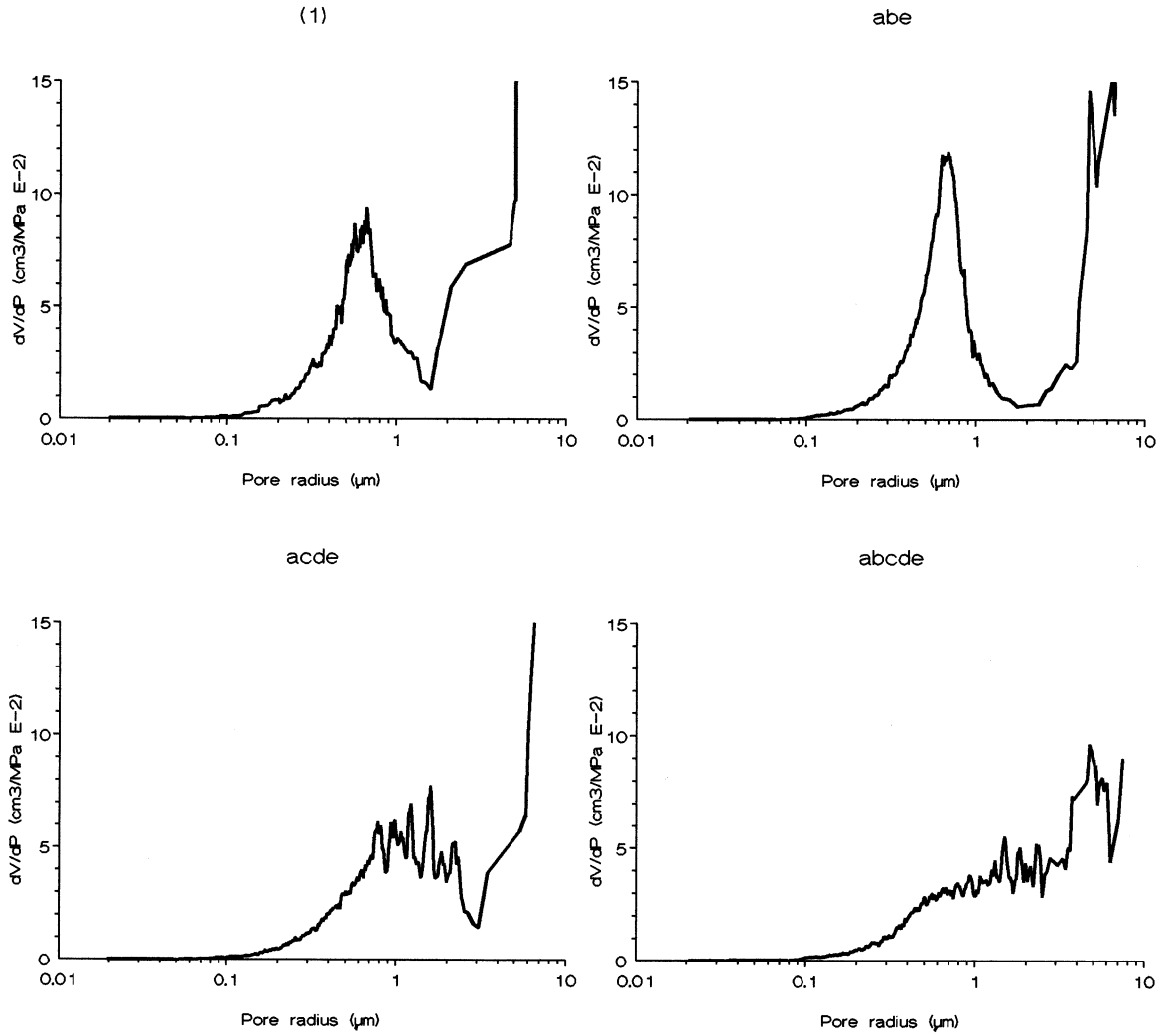

Fig. 4. dV/dP versus pore radius of pellets in the mesopore and macropore range. The volume of mercury is normalized by sample weight.

rotor speed on the specific surface area can be attributed to an effect on the geometric mean diameter.

The effects of the microcrystalline cellulose content, the rotor speed, and the spheronization time on the specific surface area can be attributed to a smoothing and pore closing effect. When spheronization went on for a longer time, open pores or surface roughnesses creating a larger surface were eliminated to a larger extent resulting in a smaller specific surface area. The interaction term ($P = 0.024$) between the microcrystalline cellulose content and the rotor speed indicates that open pores or surface roughnesses were eliminated to a larger extent when the rotor speed, i.e. the force which smooths the surface, and the microcrystalline cellulose content, i.e. the content of material which gives the pellets the ability to undergo plastic deformation when wetted, are increased simultaneously. However, also this interaction term had a major influence on the geometric mean diameter. This explains, at least

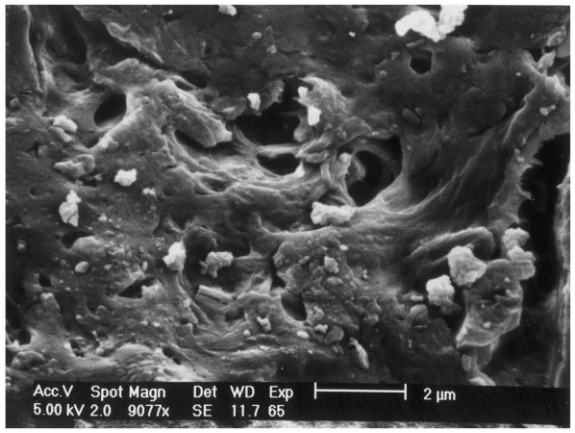

Fig. 5. SEM picture of a pellet with a small geometric mean diameter (Experiment 1, sieve fraction 180–250 μm). Magnification: $\pm 9000\times$.

partially, the effect of this interaction on the specific surface area.

3.3. Mercury porosimetry

The granule and apparent densities, porosities and volumes of mercury intruded in the different pore regions for samples of batch '(1)', 'abe', 'acde' and 'abcde' are tabulated in Table 5. The porosities indicated that all pellets contained pores with a radius <7 μm. Since apparent densities were not significantly different from the true densities as determined with a pycnometer using helium as the intrusive gas (Wilcoxon Signed Ranks tests at 95% confidence level), the volume of pores with a radius <0.02 μm was considered as being insignificant.

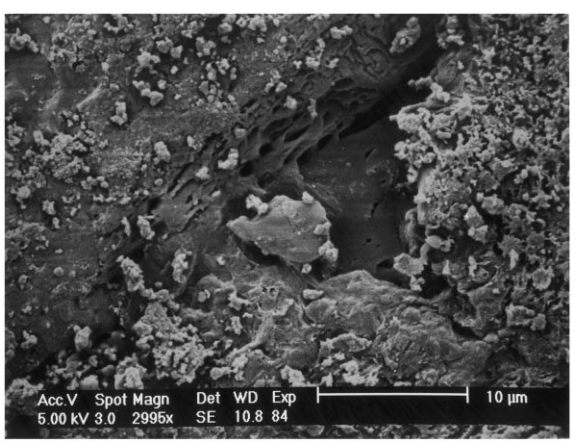

Fig. 6. SEM picture of a pellet with a large geometric mean diameter (experiment acde, sieve fraction 1180–1400 μm). Magnification: $\pm 3000\times$.

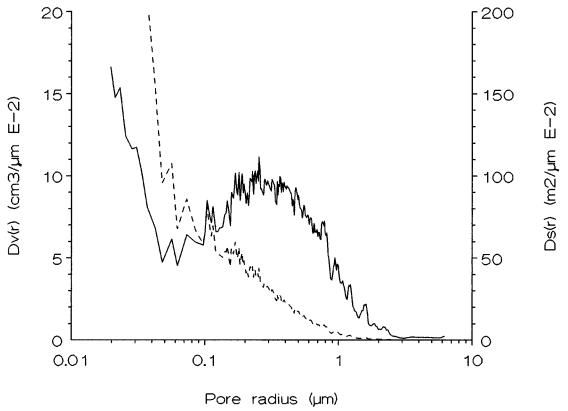

Fig. 7. $D_v(r)$ (——) and $D_s(r)$ (- - -) versus pore radius in the mesopore and macropore range (experiment acde). The volume of mercury is normalized by sample weight.

The megapore volume included large intragranular open megapores, as well as intergranular spaces. From these results, it was impossible to differentiate between them. However, with the exception of experiment '(1)', the intruded volume in the megapore range was small. The larger volume for experiment '(1)' was mainly due to the filling of the intergranular space between the small pellets with agglomerate structure (d_g of 268 μm). Moreover, no evidence for large pores with a radius of 7 μm or larger was found during SEM analysis. The mesopore volume was small for all four batches, indicating that the volume of mercury intruded in pores with a radius <0.05 μm was limited.

The mercury mainly intruded in the macropore range. For the determination of the radius at which the maximum volume intruded, the plots of dV/dP versus the pore radius were made (Fig. 4). For all samples, the largest volume of mercury intruded in the radius region of 0.1–7 μm. However, some distinctive differences were observed between the samples. The dV/dP curves as a function of the pore radius for the samples char-

acterized by the smallest size, i.e. '(1)' and 'abe', showed a sharp peak around a radius of about 0.7 μm. For the larger pellets, i.e. sample 'acde' and 'abcde', no sharp peak, but a plateau towards larger pore radii was observed.

The SEM pictures presented in Figs. 5 and 6 provide visual evidence for the presence of pores in the radius range of 0.1 to 5 μm. In Fig. 5, several pores or crevices with an outer radius of 0.1 to 1 μm are visible in a pellet characterized by a small geometric mean diameter. The smaller particles of 1 μm or less on the surface of the pellets are most likely lactose particles. In Fig. 6, a larger pore with a radius up to 5 μm can be observed in a pellet characterized by a large geometric mean diameter.

Although only four samples were investigated in terms of their pore-size distribution, thereby excluding complete statistical analysis, the results indicated that an increase in spheronization speed and time reduced the pore volume in the macropore range. An increase in amount of water when the other independent variables were set at their high level, appeared to decrease the macropore volume as well. A similar effect of increasing amount of binder solution, process speed or time on intragranular porosities, which reflects the amount of pores with a radius $< \approx 7$ μm, was reported in the literature (Jaegerskou et al., 1984; Tapper and Lindberg, 1986).

The larger pores contributed mainly to the total intruded volume, while the smaller pores had a large contribution to the surface area. This is visualised by the $D_V(r)$ and $D_S(r)$ in Fig. 7. This may explain why 'abcde' had a larger specific surface area (0.323 m^2/g) than 'acde' (0.259 m^2/g). 'abcde' had a larger pore volume in the mesopore range than 'acde', although its macropore volume was significantly (95% confidence level) smaller than the macropore volume of 'acde'.

In terms of a pellet coating process, the amount of coating material needed to obtain a certain coating thickness and thus the desired controlled release, is often based on the calculated surface area. The experiments indicate, however, that the experimentally determined specific surface areas are much larger than the calculated ones. It appears to be wise to rely on the experimentally determined surface area rather than to rely on the calculated one. However, it is probably even better to consider the pore volume, rather than the surface area. Although a surface has to be coated, one may assume that the pores with a radius between 7 and 0.05 μm are, at least partially, filled during the coating process. For example, the maximal volume that can be filled by coating materials is ≈ 80 ml per kg pellets in the case of the least porous pellets of batch 'abcde'. To fill or close these pores, a so called 'subcoat' or 'seal coat' such as a hydroxypropyl methylcellulose coat can be applied (Yang and Ghebre-Sellassie, 1990; Vuppala et al., 1997). Once the pores are filled or closed, the coating material providing the controlled release can be applied. The amount of this coating material needed to obtain a certain coating thickness can be estimated from the experimentally determined specific surface area of the seal coated pellets.

References

Eriksson, M., Nyström, C., Alderborn, G., 1993. The use of air permeametry for the assessment of external surface area and sphericity of pelletized granules. Int. J. Pharm. 99, 197–207.

Faroongsarng, D., Peck, G.E., 1994. Surface morphology study of solid powders evaluated by particle size distribution and nitrogen adsorption. Drug Dev. Ind. Pharm. 20, 2353–2367.

Holm, P., Bonde, M., Wigmore, T., 1996. Pelletization by granulation in a Roto-Processor RP-2. Part 1: Effects of process and product variables on granule growth. Pharm. Technol. Eur. 8, 22–36.

Jaegerskou, A., Holm, P., Schaefer, T., Kristensen, H.G., 1984. Granulation in high speed mixers. Part 3: Effects of process variables on the intragranular porosity. Pharm. Ind. 46, 310–314.

Juppo, A.M., Yliruusi, J., 1994. Effect of amount of granulation liquid on total pore volume and pore size distribution of lactose, glucose and mannitol granules. Eur. J. Pharm. Biopharm. 40, 299–309.

Lowell, S., Shields, J.E. (Eds.), 1991. Powder Surface Area and Porosity, 3rd Edn. Chapman and Hall, London.

Martin, A., Bustamante, P., Chun, A.H.C. (Eds.), 1993. Physical Pharmacy, 4th Edn. Lea and Febiger, Philadelphia.

Philippe, J. (Ed.), 1967. Les Méthodes Statistiques en Pharmacie et en Chimie, 1st Edn. Masson and Cie., Paris.

Schmidt, W.G., 1992. Kontrollierte Wirkstoff-Freisetzung aus Matrixpellets: geschichtete Matrizes mit Freigabe O. Ord-

nung und Initialdosis. Ph.D Thesis, Freie Universität Berlin.

Schröder, M., Kleinebudde, P., 1995. Structure of disintegrating pellets with regard to fractal geometry. Pharm. Res. 12, 1694–1700.

Tapper, G.-I., Lindberg, N.-O., 1986. The granulation of some lactose qualities with different particle size distributions in a domestic-type mixer. Acta Pharm. Suec. 23, 47–56.

Vertommen, J., Michoel, A., Rombaut, P., Kinget, R., 1994. Production of pseudoephedrine HCl pellets in a high shear mixer-granulator. Eur. J. Pharm. Biopharm. 40, 32–35.

Vertommen, J., Kinget, R., 1997. The influence of five selected processing and formulation variables on the particle size, particle size distribution, and friability of pellets produced in a rotary processor. Drug Dev. Ind. Pharm. 23, 39–46.

Vertommen, J., Rombaut, P., Kinget, R., 1997. Shape and surface smoothness of pellets made in a rotary processor. Int. J. Pharm. 146, 21–29.

Vuppala, M.K., Parikh, D.M., Bhagat, H.R., 1997. Application of powder-layering technology and film coating for manufacture of sustained-release pellets using a rotary fluid bed processor. Drug Dev. Ind. Pharm. 23, 687–694.

Wan, L.S.C., Heng, P.W.S., Liew, C.V., 1994. The role of moisture and gap air pressure in the formation of spherical granules by rotary processing. Drug Dev. Ind. Pharm. 20, 2551–2561.

Wan, L.S.C., Heng, P.W.S., Liew, C.V., 1995. The influence of liquid spray rate and atomizing pressure on the size of spray droplets and spheroids. Int. J. Pharm. 118, 213–219.

Yang, S.T., Ghebre-Sellassie, I., 1990. The effect of product bed temperature on the microstructure of Aquacoat-based controlled-release coatings. Int. J. Pharm. 60, 109–124.